



Contents lists available at [ScienceDirect](https://www.sciencedirect.com)  
**American Heart Journal Plus:**  
**Cardiology Research and Practice**

journal homepage: [www.sciencedirect.com/journal/american-heart-journal-plus-cardiology-research-and-practice](http://www.sciencedirect.com/journal/american-heart-journal-plus-cardiology-research-and-practice)



## Relationship of high-intensity plaques on T1-weighted magnetic resonance imaging with coronary intraplaque hemorrhage: A directional coronary atherectomy study

Shoichi Ehara<sup>a,\*</sup>, Kazuki Mizutani<sup>a</sup>, Takanori Yamazaki<sup>a</sup>, Kenji Matsumoto<sup>a</sup>, Tsukasa Okai<sup>a</sup>, Tomohiro Yamaguchi<sup>a</sup>, Yasuhiro Izumiya<sup>a</sup>, Takahiko Naruko<sup>b</sup>, Minoru Yoshiyama<sup>a</sup>

<sup>a</sup> Department of Cardiovascular Medicine, Osaka City University Graduate School of Medicine, Osaka, Japan

<sup>b</sup> Department of Cardiology, Osaka City General Hospital, Osaka, Japan

### ARTICLE INFO

#### Keywords:

Coronary artery disease  
 Magnetic resonance imaging  
 Atherectomy  
 Atherosclerosis  
 Macrophage

### ABSTRACT

**Background:** Although intraplaque hemorrhage (IPH) has been identified as a key feature of rupture-prone plaques, noninvasive imaging-based features for its detection in coronary artery have not been clearly established. The aim of this study was to investigate the relationship of the ratio between the signal intensities of coronary plaque and cardiac muscle (PMR) on non-contrast T1-weighted imaging (T1WI) in magnetic resonance with IPH in the directional coronary atherectomy (DCA) specimens.

**Methods:** Fifteen lesions from 15 patients, who underwent DCA and T1WI, were prospectively enrolled. The snap-frozen samples obtained by DCA were used for immunohistochemical staining against a protein specific to erythrocyte membranes (glycophorin A) and macrophages. The percentage of glycophorin A and macrophages was graded using a scale from 0 to 4, with higher scores indicating higher percentages.

**Results:** PMR showed a strong positive correlation with glycophorin A scores ( $\rho = 0.772$ ,  $p < 0.001$ ), whereas, there was a weak correlation between the PMR and macrophage scores ( $\rho = 0.626$ ,  $p < 0.05$ ). The receiver-operating characteristic curve analysis showed that the optimal PMR cutoff value for predicting glycophorin A scores  $\geq$  grade 2 (glycophorin A-positive area  $\geq 5\%$  of the plaque) was 1.2 (area under the curve; 0.91, 95% confidence interval; 0.73–1.00), and this PMR value had a sensitivity of 8/9 (89%), specificity of 6/6 (100%), positive predictive value of 8/8 (100%), and negative predictive value of 6/7 (86%).

**Conclusions:** In patients with ischemic heart disease, a high PMR on T1WI is a predictor of coronary IPH as assessed by DCA specimens.

### 1. Introduction

Pathological studies have shown that plaque rupture or erosion of the endothelial surface with subsequent thrombus formation are the most important mechanisms in acute coronary syndromes [1–3]. A large lipid-pool, thin-cap fibroatheroma, macrophage accumulation, and intraplaque hemorrhage (IPH) have been identified as the key features of rupture-prone plaques [4]. Among these vulnerable plaque characteristics, IPH has been associated with more rapid growth of the lipid

core and accelerated enlargement of the plaque size, resulting in luminal narrowing [5,6]. Nevertheless, noninvasive imaging-based features for detecting IPH in the coronary artery have not been clearly established.

Over the past several decades, non-contrast T1-weighted imaging (T1WI) in magnetic resonance (MR) has emerged as a novel plaque imaging technique. Pathohistological studies using carotid endarterectomy specimens demonstrated that high-intensity plaques (HIPs) in the carotid arterial wall on T1WI indicate the presence of IPH-containing methemoglobin [7–9]. Recently, coronary plaque imaging by T1WI

**Abbreviations:** IPH, intraplaque hemorrhage; T1WI, T1-weighted imaging; MR, magnetic resonance; HIP, high-intensity plaque; PMR, the ratio between the signal intensities of coronary plaque and cardiac muscle; IVUS, intravascular ultrasound; OCT, optical coherence tomography; DCA, directional coronary atherectomy; PCI, percutaneous coronary intervention; ROC, receiver-operating characteristic.

\* Corresponding author at: Department of Cardiovascular Medicine, Osaka City University Graduate School of Medicine, 1-4-3 Asahi-machi, Abeno-ku, Osaka 545-8585, Japan.

E-mail address: [ehara@med.osaka-cu.ac.jp](mailto:ehara@med.osaka-cu.ac.jp) (S. Ehara).

<https://doi.org/10.1016/j.ahjo.2021.100047>

Received 10 April 2021; Received in revised form 28 May 2021; Accepted 24 August 2021

Available online 6 October 2021

2666-6022/© 2021 The Authors.

Published by Elsevier Inc.

This is an open access article under the CC BY-NC-ND license

(<http://creativecommons.org/licenses/by-nc-nd/4.0/>).

has also been successfully applied with respiratory gating techniques [10–13]. Some groups, including ours, reported that coronary artery HIPs, determined by the ratio between the signal intensities of coronary plaque and cardiac muscle (PMR), are associated with vulnerable plaque characteristics detected by various imaging modalities such as intravascular ultrasound (IVUS) and optical coherence tomography (OCT) [10–12]. Moreover, the presence of plaques with high PMR on T1WI was a significant and independent predictor of future coronary events in patients with coronary artery disease [13]. However, the association between HIPs and specimens directly obtained from *in vivo* coronary plaques has not been investigated. Therefore, the precise plaque morphology of coronary HIPs is still unknown.

Coronary atherectomy specimens, a unique source of plaque tissue, provide precise histological details regarding plaque morphology *in vivo*, which has the potential for improving our understanding of HIPs on T1WI. Accordingly, the aim of this study was to investigate the association between PMR on non-contrast T1WI and IPH in the coronary atherectomy specimens.

## 2. Methods

### 2.1. Study design and participants

Between May 2017 and August 2019, a total of 16 patients, who underwent directional coronary atherectomy (DCA) of a native “*de novo*” atherosclerotic lesion and MR, were prospectively enrolled in this study. A bypass graft or restenotic lesion after percutaneous coronary intervention (PCI) was not included in this study. After coronary angiography, patients were selected for DCA using strictly defined angiographic criteria: a proximally located eccentric target lesion in a non-tortuous coronary artery  $\geq 3$  mm in diameter, particularly bifurcated lesions including left main trunk, ostial left anterior descending coronary artery, ostial left circumflex coronary artery and ostial right coronary artery [14]. All patients underwent MR within 7 days ( $2 \pm 1$  days) before DCA was performed. Among the 16 subjects enrolled initially, one was excluded from the final analysis because a specimen was not obtained. Finally, 15 lesions from 15 patients, who presented with unstable angina pectoris ( $n = 1$ ), stable angina pectoris ( $n = 7$ ), or silent myocardial ischemia ( $n = 7$ ) were examined in this study. The target vessel was identified based on clinical and angiographic data in a patient with unstable angina and was considered as an ischemia-related vessel identified on a scintigram stress test in patients with stable angina or silent myocardial ischemia. Oral aspirin (100 mg) and clopidogrel (75 mg) or prasugrel (3.75 mg) were administered on admission.

The study was approved by the hospital ethics committee (approval no.2020-019).

### 2.2. MR coronary plaque image acquisition and analysis

Coronary plaque imaging was performed using a 1.5-T MR imager (Achieva, Philips Medical Systems) with a 32-element cardiac coil. Initial survey images were focused around the heart, following which the reference images were obtained for the sensitivity of parallel imaging. Transaxial cine MR images were then acquired using a steady-state free-precession sequence with breath holding, to determine the trigger delay time when the motion of the right coronary artery was minimal.

First, to obtain detailed information on the location of the target lesion, free-breathing, steady-state, free-precession, whole-heart coronary MR angiographic images were obtained (repetition time, 3.7 ms; echo time, 1.8 ms; flip angle,  $80^\circ$ ; SENSE factor, 2.0; number of excitations, 1; navigator gating window of  $\pm 2.0$  mm with diaphragm drift correction; field of view,  $300 \times 255 \times 120$  mm [rectangular field of view, 85%]; acquisition matrix,  $240 \times 240$ ; reconstruction matrix,  $512 \times 512 \times 160$ , resulting in an acquired spatial resolution of  $1.25 \times 1.25 \times 1.5$  mm reconstructed to  $0.6 \times 0.6 \times 0.75$  mm).

Next, coronary plaque images were obtained while the patients were breathing freely, by using a three-dimensional T1WI, inversion-recovery, gradient-echo technique with fat-suppressed and radial k-space sampling in the Y-Z plane (repetition time, 4.4 ms; echo time, 2.0 ms; flip angle,  $20^\circ$ ; SENSE factor, 2.5; number of excitations, 2; navigator gating window of  $\pm 1.5$  mm with diaphragm drift correction; field of view,  $300 \times 240 \times 120$  mm [rectangular field of view, 80%]; acquisition matrix,  $224 \times 224$ ; reconstruction matrix,  $512 \times 512 \times 140$ , resulting in an acquired spatial resolution of  $1.34 \times 1.34 \times 1.7$  mm reconstructed to  $0.6 \times 0.6 \times 0.85$  mm). The inversion time of the inversion-recovery sequence was adjusted to null blood signal by using a Look-Locker sequence [12].

The location of the target lesion was determined by carefully comparing the coronary angiographic and MR angiographic images by using fiduciary points such as side branches. Once the target lesion had been confirmed on coronary MR angiography, the areas corresponding to the above site in coronary T1WI were carefully matched according to the surrounding cardiac and chest wall structures. PMR was then calculated as the highest signal intensity of the coronary plaque divided by the signal intensity of the left ventricular muscle near the coronary plaque, measured by placing a manually freehand circular region of interest on a standard console of the clinical MR system, in accordance with previous reports [10–13]. The MR coronary image dataset was analyzed by a single investigator (S.E.) who was blinded to the patients' pathohistological data. The interobserver variability for measurement of the PMR performed in a random sample of patients previously was  $5.8 \pm 3.9\%$  ( $r^2 = 0.968$ ,  $p < 0.0001$ ).

### 2.3. Directional coronary atherectomy and specimen pretreatment

Atherectomy was performed with a femoral approach using an 8-Fr arterial sheath and guide catheter and DCA (ATHEROCUT, Nipro Co.). Immediately after atherectomy, the tissue specimens were carefully oriented along their longest axis, snap-frozen, and stored at  $-80^\circ\text{C}$ . Subsequently, the snap-frozen samples obtained by DCA were serially sectioned to produce 5- $\mu\text{m}$  sections, which were then fixed in acetone. The first section was stained with hematoxylin-eosin. The other sections were used for immunohistochemical staining [15].

### 2.4. Immunohistochemistry

The cellular components were analyzed using monoclonal antibodies against macrophages (EBM11, DAKO) and a protein specific to erythrocyte membranes (Glycophorin A, DAKO). Non-immune mouse IgG serum (DAKO) served as a negative control. Sections were incubated at  $4^\circ\text{C}$  overnight or for 1 h at room temperature, and then subjected to a three-step staining procedure, using the streptavidin-biotin complex method for detection [15].

### 2.5. Quantitative methods

The tissue area occupied by immunostained glycophorin A and macrophages was quantified using computer-aided planimetry and expressed as a percentage of the total surface area of the tissue section. On the basis of the percentage of glycophorin A and macrophages, scores were assigned from 0 to 4 as follows according to a previous report [5]: 0 indicates no detectable staining; 1 indicates focal granular staining in  $<5\%$  of the plaque; 2 indicates mild granular staining in 5 to 10% of the plaque; 3 indicates moderate granular staining in 11–25% of the plaque; and 4 indicates marked granular staining in  $>25\%$  of the plaque. Morphometric analysis was performed by a single investigator (T.N.) who was blinded to the patients' characteristics and clinical data.

### 2.6. Statistical analyses

Continuous data are presented as the mean  $\pm$  standard deviation or

median and interquartile range for non-normally distributed data. PMR did not distribute normally; therefore, a transformed logarithmic value was used for the following analyses. Correlations among continuous variables were assessed with the use of the Spearman rank-correlation coefficient. Receiver-operating characteristic (ROC) curve analysis was used to assess the cutoff values of PMR to predict glycoporphin A scores  $\geq$  grade 2 at the highest possible sensitivity and specificity levels. All analyses were performed using JMP statistical software version 10 (SAS Institute Inc., Cary, NC, USA) and SPSS version 22.0 (SPSS, Chicago, IL, USA), and *p*-values  $<0.05$  were considered significant.

### 3. Results

All DCA procedures were successfully performed without any serious complications. Subsequent to DCA, 7 patients (46.7%) underwent drug-eluting stents implantation; PCI was completed without stent implantation (DCA alone or drug-coated balloon) in 8 patients (53.3%). Clinical characteristics of all patients are shown in Table 1. The mean age of the study cohort was  $67 \pm 11$  years, and most patients were men. Most target lesions were observed in the proximal left anterior descending artery; no patients had the target lesion in the left circumflex coronary artery. The median value of PMR was 1.2.

Fig. 1 shows the correlation between PMR and the glycoporphin A or macrophage scores. PMR showed a positive correlation with glycoporphin A scores ( $\rho = 0.772$ ,  $p < 0.001$ ; Fig. 1-A), whereas, there was a weak correlation between PMR and macrophage scores ( $\rho = 0.626$ ,  $p < 0.05$ ; Fig. 1-B). A significant positive correlation was noted between the scores of glycoporphin A and macrophages ( $\rho = 0.590$ ,  $p < 0.05$ ; Fig. 1-C). The linear regression analysis was performed to identify the factors associated with glycoporphin A scores (Table 2). Among the clinical covariates, PMR ( $p < 0.01$ ) and smoking ( $p < 0.05$ ) were associated with a higher glycoporphin A score. The ROC analysis showed that the optimal PMR cutoff value for predicting glycoporphin A scores  $\geq$  grade 2 (glycoporphin A-positive area  $\geq 5\%$  of the plaque) was 1.2 (area under the curve, 0.91; 95% confidence interval, 0.73–1.00). This PMR value had a sensitivity of 8/9 (89%), specificity of 6/6 (100%), positive predictive value of 8/8 (100%), and negative predictive value of 6/7 (86%). Moreover, the additional MR plaque image analysis performed by another independent observer (K.M.) showed that sensitivity, specificity, positive predictive value, and negative predictive value of the PMR of 1.2 to predict glycoporphin A scores  $\geq$  grade 2 determined above

analysis, were 8/9 (89%), 5/6 (83%), 8/9 (89%), and 5/6 (83%), respectively. A representative case of HIP on T1WI in comparison with plaque morphology in the atherectomy specimen is shown in Fig. 2-A. In the lesion with a high PMR (PMR = 1.41), immunostaining for erythrocytes (glycophorin A) revealed that abundant erythrocytes were found in the area of macrophage accumulation. In contrast, Fig. 2-B shows a case with a non-HIP lesion (PMR = 0.63). The atherectomy specimens contained white plaques and scattered macrophages, but no erythrocytes.

### 4. Discussion

To the best of our knowledge, this is the first study to show the significant association between a high PMR on non-contrast T1WI and IPH in coronary atherectomy specimens.

Since the introduction of non-contrast T1WI on MR for plaque imaging, the usefulness of this tool has predominantly been investigated for carotid arteries. In comparative studies using carotid atherectomy specimens, many researchers showed that HIPs in the carotid arterial wall on T1WI related to the presence of IPH-containing methemoglobin [7–9] and cerebral ischemia. Although the significant association between HIP on T1WI and intracoronary thrombus detected by invasive CAG [16] and OCT [11] has been shown in the previous studies, the role of HIP in the prediction of IPH in coronary arteries remains uncertain. Recent studies showed the close relationship of HIP presence with vulnerable plaque characteristics detected by multislice computed tomography, IVUS, and OCT [10–12]. Regrettably, these current imaging techniques do not allow a definitive discrimination between haemorrhages and lipid components. Therefore, the current study aimed to test whether HIP indicates IPH seen in the pathohistological specimens from coronary, rather than carotid, arteries.

To date, few comparisons with pathohistological data have been performed in coronary artery studies. Liu et al. investigated the association between HIPs on T1WI and the presence of IPH through *ex vivo* imaging of both carotid and coronary plaque specimens, obtained during coronary artery bypass grafting [17]. Unfortunately, no coronary artery plaques had IPH in this study, although carotid HIPs were shown to be associated with the presence of IPH. More recently, Kuroiwa et al. demonstrated that HIPs defined as PMR  $\geq 1.4$  may reflect IPH in coronary arteries from autopsy cases [18]. However, no direct comparisons with pathohistological data have been performed in living patients. We first show that a higher PMR correlated with higher glycoporphin A scores indicating greater proportions of erythrocytes in the coronary atherectomy specimens.

There was a significant positive correlation between the scores of glycoporphin A and macrophages. This finding is consistent with several lines of evidence, which show that an increase in the amount of lipid core, mechanical stresses, and overproduction of oxygen free radicals by macrophages could lead to the breakdown of microvessels and IPH production [5,6]. Findings from previous reports [8,18] indicate that the presence of IPH associated with inflammation may be related to HIP on T1WI.

The findings of the present study are clinically significant. First, the detection of IPH represented by HIP in coronary arteries would alert the clinician to the possibility of plaque instability. The PMR of 1.2 was the best cutoff value for the prediction of glycoporphin A scores  $>$  grade 2 as a representative of IPH regardless of the clinical symptom. This finding is consistent with our recent study reported that the optimal PMR cutoff value for predicting OCT defined intracoronary thrombus was 1.2 [12]. Therefore, patients with HIP should be recognized as high risk including subclinical IPH. Moreover, it should be noted that higher the PMR, greater is the accumulation of glycoporphin A. Kolodgie et al. showed that glycoporphin A score of grade 4 was associated with markedly larger size of necrotic core than that of grade 3 or less [5]. Thus, HIP with much higher PMR might be associated with the large necrotic core which was frequently observed in patients with acute coronary syndrome. A recent

**Table 1**

Clinical characteristics.

	<i>n</i> = 15
PMR	1.19 (0.81–1.41)
Age, yrs	$67.4 \pm 10.7$
Female	2 (13%)
Hypertension	6 (40%)
Dyslipidemia	10 (67%)
Diabetes mellitus	3 (20%)
Smoking	4 (27%)
Target vessel	
Left main trunk	1 (7%)
Left anterior descending artery	13 (86%)
Left circumflex artery	0 (0%)
Right coronary artery	1 (7%)
Medication	
Calcium channel blocker	5 (33%)
ACEi/ARB	7 (47%)
Beta blocker	7 (47%)
Statin	12 (80%)
Percent diameter stenosis	$65.3 \pm 5.5$

Values are the *n* (%), mean  $\pm$  standard deviation, or median (interquartile range).

PMR, the ratio between the signal intensities of coronary plaque and cardiac muscle; ACEi, angiotensin converting enzyme inhibitor; ARB, angiotensin receptor blocker.

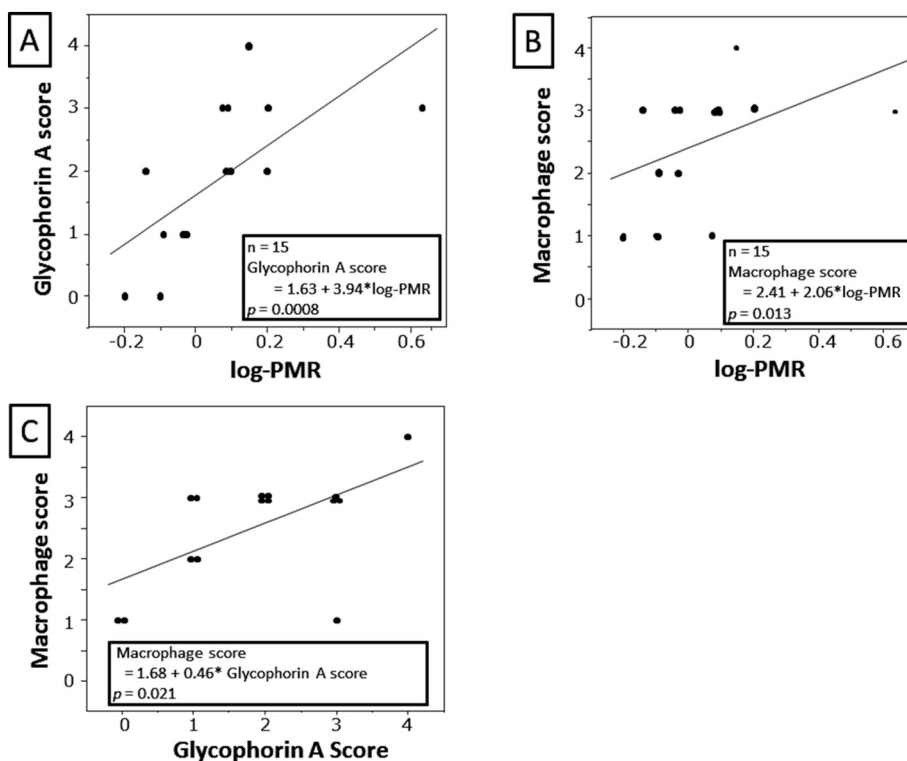


**Fig. 1.** (A) Correlation between the ratio of the signal intensities of the coronary plaque and cardiac muscle (PMR) and glycophorin A scores. (B) Correlation between PMR and macrophage scores. (C) Correlation between glycophorin A and macrophage scores. Scores can range from 0 to 4, with higher scores indicating greater proportions of glycophorin A or macrophages.

**Table 2**  
Linear regression analysis for factors associated with glycophorin A scores.

	$\beta$ (SE)	p-value
Log-PMR	0.66 (1.24)	0.0072
Age	-0.21 (0.030)	0.44
Female	0.22 (0.46)	0.44
Hypertension	0.095 (0.32)	0.74
Dyslipidemia	0.29 (0.32)	0.30
Diabetes mellitus	-0.087 (0.40)	0.76
Smoking	-0.59 (0.29)	0.021
Left anterior descending artery	0.30 (0.45)	0.28
Medication		
Calcium channel blocker	-0.041 (0.34)	0.88
ACEi/ARB	-0.12 (0.32)	0.66
Beta blocker	0.11 (0.32)	0.70
Statin	-0.20 (0.39)	0.47

PMR, the ratio between the signal intensities of coronary plaque and cardiac muscle; ACEi, angiotensin converting enzyme inhibitor; ARB, angiotensin receptor blocker; SE, standard errors.

study demonstrated that the PMR was lowered by statin therapy, which was also associated with decrease in low-density lipoprotein-cholesterol and high-sensitivity C-reactive protein levels as well as a decrease in plaque volume on computed tomography angiography [19]. Accordingly, in the future, IPH detected by T1WI may be a potential therapeutic target to prevent cardiovascular events. In addition, several studies have demonstrated that the presence of HIP has the potential to predict myocardial injury during PCI, which is associated with worse short-term and long-term clinical outcomes [20,21]. Although the etiology of PCI-related myocardial injury is a multifactorial phenomenon, the predominant mechanism involves the distal embolization of atheromatous or thrombotic materials, and results from the mechanical fragmentation of the culprit plaque during PCI [22]. Taken together, further prospective randomized trials should be conducted in order to examine whether

distal protection devices might prevent myocardial injury during PCI for patients with higher PMR.

**5. Limitations**

This study had some limitations. First, in the present DCA analysis, the number of samples (n = 15) is too small to perform multivariate analysis. Further studies with more cases will be needed to confirm the present results. Nevertheless, a pathohistological approach using DCA specimens is acknowledged as the only reliable method for the assessment of *in vivo* coronary plaque characteristics. Therefore, we consider the quality of our data obtained using both coronary MR imaging and DCA specimens as sufficiently high to validate our conclusion. Second, all target lesions except one HIP were present in the proximal left anterior descending artery. Therefore, our results were also limited by selection bias.

**6. Conclusions**

In patients with ischemic heart disease, a high PMR on T1WI represents coronary IPH as assessed using DCA specimens. This finding may provide insights to further our understanding of coronary IPH.

**CRedit authorship contribution statement**

Shoichi Ehara: Methodology and Writing-original draft. Kazuki Mizutani: Investigation. Takanori Yamazaki: Data curation. Tsukasa Okai: Data curation. Tomohiro Yamaguchi: Data curation. Takahiko Naruko: Formal analysis. Kenji Mastumoto: Writing-review & editing. Yasuhiro Izumiya: Supervision. Minoru Yoshiyama: Supervision.

**Grant supporting this paper**

This work was supported by a grant from the Japan Society for the

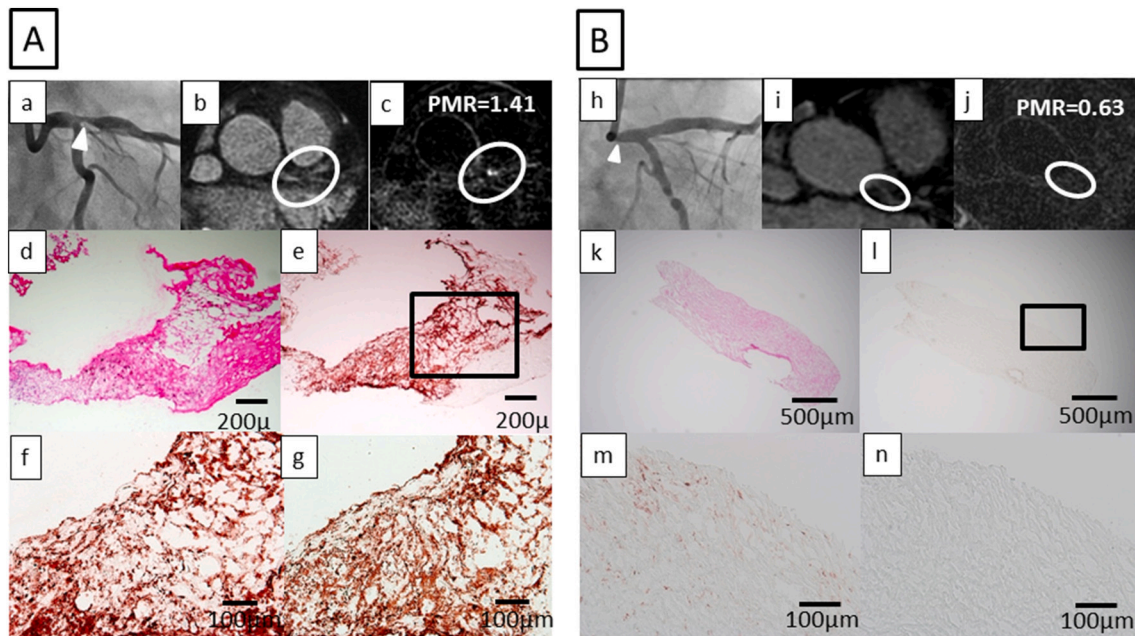


**Fig. 2.** (A) A representative case of a high-intensity plaques (HIP) on T1-weighted imaging (T1WI) in comparison with plaque morphology in an atherectomy specimen. a, Coronary angiography revealed severe coronary stenosis in the proximal left anterior descending artery (arrowhead). b, Whole-heart coronary MR angiography showed severe stenosis in the proximal left anterior descending artery (circle). c, Coronary T1WI demonstrated HIP (circle). The value of PMR was 1.41. d-g, Micrographs of an atherectomy specimen obtained from a target lesion. d, Hematoxylin-eosin stained section. e, The adjacent section stained with an anti-glycophorin A antibody revealed the presence of abundant glycophorin A-positive cells. The boxed area is enlarged in f and g. f, Anti-CD68 antibody staining showed macrophage accumulation. g, Anti-glycophorin A antibody staining revealed the presence of abundant glycophorin A-positive cells. Bar: d, e, 200  $\mu$ m. f, g, 100  $\mu$ m.

(B) A representative case of a non-HIP lesion on T1WI in comparison with plaque morphology in an atherectomy specimen. h, Coronary angiography revealed moderate coronary stenosis in the ostium of the left main coronary artery (arrowhead). i, Whole-heart coronary MR angiography showed significant stenosis in the ostium of the left main coronary artery (circle). j, Coronary T1WI revealed a low-intensity plaque (circle). The value of PMR was 0.63. k-n, Micrographs of an atherectomy specimen obtained from a target lesion. k, Hematoxylin-eosin stained section. l, The adjacent section stained with an anti-glycophorin A antibody revealed no glycophorin A-positive cells. The boxed area is enlarged in m and n. m, Anti-CD68 antibody staining revealed scattered macrophages. n, Anti-glycophorin A antibody staining revealed no glycophorin A-positive cells. Bar: k, l, 500  $\mu$ m. m, n, 100  $\mu$ m.

Promotion of Science (JSPS) KAKENHI Grant Number 20K22882.

### Declaration of competing interest

The authors report no relationships that could be construed as a conflict of interest.

### References

- V. Fuster, L. Badimon, J.J. Badimon, J.H. Chesebro, The pathogenesis of coronary artery disease and the acute coronary syndromes, *N. Engl. J. Med.* 326 (242–250) (1992) 310–318, <https://doi.org/10.1056/NEJM199201233260406>.
- A.C. van der Wal, A.E. Becker, C.M. van der Loos, P.K. Das, Site of intimal rupture or erosion of thrombosed coronary atherosclerotic plaques is characterized by an inflammatory process irrespective of dominant plaque morphology, *Circulation* 89 (1994) 36–44, <https://doi.org/10.1161/01.cir.89.1.36>.
- R. Virmani, F.D. Kolodgie, A.P. Burke, A. Farb, S.M. Schwartz, Lessons from sudden coronary death: a comprehensive morphological classification scheme for atherosclerotic lesions, *Arterioscler. Thromb. Vasc. Biol.* 20 (2000) 1262–1275, <https://doi.org/10.1161/01.atv.20.5.1262>.
- A.V. Finn, M. Nakano, J. Narula, F.D. Kolodgie, R. Virmani, Concept of vulnerable/unstable plaque, *Arterioscler. Thromb. Vasc. Biol.* 30 (2010) 1282–1292, <https://doi.org/10.1161/ATVBAHA.108.179739>.
- F.D. Kolodgie, H.K. Gold, A.P. Burke, et al., Intraplaque haemorrhages and progression of coronary atherosclerosis, *N. Engl. J. Med.* 349 (2003) 2316–2325, <https://doi.org/10.1056/NEJMoa035655>.
- J.B. Michel, R. Virmani, E. Arbustini, G. Pasterkamp, Intraplaque haemorrhages as the trigger of plaque vulnerability, *Eur. Heart J.* 32 (2011) 1977–1985, <https://doi.org/10.1093/eurheartj/ehr054>.
- A.R. Moody, R.E. Murphy, P.S. Morgan, et al., Characterization of complicated carotid plaque with magnetic resonance direct thrombus imaging in patients with cerebral ischemia, *Circulation* 107 (2003) 3047–3052, <https://doi.org/10.1161/01.CIR.0000074222.61572.44>.
- N. Takaya, C. Yuan, B. Chu, et al., Presence of intraplaque hemorrhage stimulates progression of carotid atherosclerotic plaques: a high-resolution magnetic resonance imaging study, *Circulation* 111 (2005) 2768–2775, <https://doi.org/10.1161/CIRCULATIONAHA.104.504167>.
- J. Sun, H.R. Underhill, D.S. Hippe, Y. Xue, C. Yuan, T.S. Hatsukami, Sustained acceleration in carotid atherosclerotic plaque progression with intraplaque hemorrhage, *JACC Cardiovasc. Imaging* 5 (2012) 798–804, <https://doi.org/10.1016/j.jcmg.2012.03.014>.
- T. Kawasaki, S. Koga, N. Koga, et al., Characterization of hyperintense plaque with noncontrast T1-weighted cardiac magnetic resonance coronary plaque imaging: comparison with multislice computed tomography and intravascular ultrasound, *JACC Cardiovasc. Imaging* 2 (2009) 720–728, <https://doi.org/10.1016/j.jcmg.2009.01.016>.
- S. Ehara, T. Hasegawa, S. Nakata, et al., Hyperintense plaque identified by magnetic resonance imaging relates to intracoronary thrombus as detected by optical coherence tomography in patients with angina pectoris, *Eur. Heart J. Cardiovasc. Imaging* 13 (2012) 394–399, <https://doi.org/10.1093/ehjci/jer305>.
- K. Matsumoto, S. Ehara, T. Hasegawa, et al., Localization of coronary high-intensity signals on T1-weighted MR imaging: relation to plaque morphology and clinical severity of angina pectoris, *JACC Cardiovasc. Imaging* 8 (2015) 1143–1152, <https://doi.org/10.1016/j.jcmg.2015.06.013>.
- T. Noguchi, T. Kawasaki, A. Tanaka, et al., High-intensity signals in coronary plaques on non-contrast T1-weighted magnetic resonance imaging as a novel determinant of coronary events, *J. Am. Coll. Cardiol.* 63 (2014) 989–999, <https://doi.org/10.1016/j.jacc.2013.11.034>.
- E. Tsuchikane, T. Aizawa, H. Tamai, et al., Pre-drug-eluting stent debulking of bifurcated coronary lesions, *J. Am. Coll. Cardiol.* 50 (2007) 1941–1945, <https://doi.org/10.1016/j.jacc.2007.07.066>.
- K. Yunoki, T. Naruko, R. Komatsu, et al., Enhanced expression of haemoglobin scavenger receptor in accumulated macrophages of culprit lesions in acute coronary syndromes, *Eur. Heart J.* 30 (2009) 1844–1852, <https://doi.org/10.1093/eurheartj/ehp257>.
- C.H.P. Jansen, D. Perera, M.R. Makowski, et al., Detection of intracoronary thrombus by magnetic resonance imaging in patients with acute myocardial infarction, *Circulation* 124 (2011) 416–424, <https://doi.org/10.1161/CIRCULATIONAHA.110.965442>.
- W. Liu, Y. Xie, C. Wang, et al., Atherosclerosis T1-weighted characterization (CATCH): evaluation of the accuracy for identifying intraplaque hemorrhage with histological validation in carotid and coronary artery specimens, *J. Cardiovasc. Magn. Reson.* 20 (2018) 27, <https://doi.org/10.1186/s12968-018-0447-x>.

- [18] Y. Kuroiwa, A. Uchida, A. Yamashita, et al., Coronary high-signal-intensity plaques on T1-weighted magnetic resonance imaging reflect intraplaque hemorrhage, in: *Cardiovascular. Pathology* 40, 2019, pp. 24–31, <https://doi.org/10.1016/j.carpath.2019.01.002>.
- [19] T. Noguchi, A. Tanaka, T. Kawasaki, et al., Effect of intensive statin therapy on coronary high-intensity plaques detected by noncontrast T1-weighted imaging: the AQUAMARINE pilot study, *J. Am. Coll. Cardiol.* 66 (2015) 245–256, <https://doi.org/10.1016/j.jacc.2015.05.056>.
- [20] T. Hoshi, A. Sato, D. Akiyama, et al., Coronary high-intensity plaque on T1-weighted magnetic resonance imaging and its association with myocardial injury after percutaneous coronary intervention, *Eur. Heart J.* 36 (2015) 1913–1922, <https://doi.org/10.1093/eurheartj/ehv187>.
- [21] K. Matsumoto, S. Ehara, T. Hasegawa, K. Otsuka, J. Yoshikawa, K. Shimada, Prediction of the filter no-reflow phenomenon in patients with angina pectoris by using multimodality: magnetic resonance imaging, optical coherence tomography, and serum biomarkers, *J. Cardiol.* 67 (2016) 430–436, <https://doi.org/10.1016/j.jjcc.2015.06.015>.
- [22] S. Kaul, The “no reflow” phenomenon following acute myocardial infarction: mechanisms and treatment options, *J. Cardiol.* 64 (2014) 77–85, <https://doi.org/10.1016/j.jjcc.2014.03.008>.